



Evaluation of surface quality and mechanical properties of squeeze casted AA2026 aluminum alloy using response surface methodology

Muhammad Asad Ali¹ · Kashif Ishfaq² · Muhammad Jawad¹

Received: 21 February 2019 / Accepted: 30 April 2019 / Published online: 16 May 2019
© Springer-Verlag London Ltd., part of Springer Nature 2019

Abstract

Aluminum–copper alloys are widely employed in automobile and aerospace industries owing to their marvelous mechanical and physical attributes. But the major hindrance in their application is that these materials are more susceptible to casting defects such as porosity, hot tears, and shrinkage occurring during solidification. The said issues have a negative impact on the mechanical properties of the casted materials and thus limit their use. Squeeze casting is a promising choice for these materials that has an ability to manufacture near-net shape parts with superior surface finish and better mechanical properties. Although, the potential of this method is tested for a variety of materials, but its capability for casting AA2026 alloy is yet to be comprehensively explored which is the primary focus of this research. Three key parameters of squeeze casting process, namely squeeze pressure, die temperature, and pouring temperature are selected for investigating their influence on surface roughness, ultimate tensile strength, and hardness using response surface methodology. Experimental results are analyzed using analysis of variance to find the control factor's significance and adequacy of models. It has been found that squeeze pressure is the most influencing parameter for surface roughness whereas for ultimate tensile strength and hardness, pouring temperature is the major contributing factor. SEM analysis is carried out to reveal the micro-details of the fractured samples. In addition to finding optimal ranges of control variables (using contour plot analysis) for each response individually, a multi-response optimization has also been carried out using desirability approach. Furthermore, mathematical models are also developed and validated through confirmatory tests. The results of confirmatory runs depict that the proposed models have a high degree of prediction accuracy.

Keywords Squeeze casting · Aluminum alloy 2026 · Mechanical properties · Surface quality · Response surface methodology

1 Introduction

Aluminum and its alloys are commonly used in various applications like aerospace and automotive because of having better mechanical properties, excellent strength, better formability characteristics, and being light weight as well [1–5].

Aluminum AA2026 is the mainstream alloy in both the aforesaid industrial applications. This alloy has 3.6–4.3% Cu along with other elements that enhances its fatigue performance, damage tolerance, fracture toughness, tensile strength, and surface finish [6, 7]. Components used in automotive and aerospace applications have complex geometries, and it is essential for the sustainability of these geometries that their surface should be free from defects. Moreover, the components should have high strength and better surface finish. These characteristics cannot be achieved by traditional casting because these processes generate defects [8, 9]. Squeeze casting (a non-traditional casting technique) is a promising choice for such applications. In this method, liquidus metallic material is poured into the die cavity under high pressure. Solidification occurs under pressure which provides higher surface finish and better mechanical properties [10, 11].

Quality of products made by squeeze casting primarily depends upon mechanical properties and surface finish. Both the said attributes are prominently pretentious by input parameters

✉ Kashif Ishfaq
Kashifishfaq1@gmail.com

Muhammad Asad Ali
asadaliuetian@gmail.com

Muhammad Jawad
jawad@uettaxila.edu.pk

¹ Department of Industrial Engineering, University of Engineering and Technology Taxila, Rawalpindi, Pakistan

² Department of Industrial and Manufacturing Engineering, University of Engineering and Technology Lahore, Lahore 54890, Pakistan

like squeeze pressure (S_p), die temperature (D_T), pouring temperature (P_T), and die material [12–14]. Patel et al. [15] concluded that surface roughness (SR) was significantly affected by the change in the value of squeeze pressure. It was also claimed that optimized value of surface roughness was achieved at S_p of 120 MPa, D_T of 225 °C, and P_T of 720 °C. Senthil and Amirthagadeswaran [16] observed that optimized ultimate tensile strength (UTS) was obtained at S_p of 100 MPa, P_T of 725 °C, D_T of 200 °C, and pressure duration of 45 s. Furthermore, all the narrated parameters were proved to have a significant effect on UTS and hardness. Souissi et al. [17] found that UTS and yield strength was impressively improved with the increase in squeeze pressure during squeeze casting of AA2017 aluminum alloy. Bin et al. [18] determined that UTS of AlSi₉Cu₃ alloy was decreased by increasing the pouring temperature and pressure. It was reported that magnitude of UTS and hardness was increased by 16.7% and 10.1%, respectively, in comparison with that found in sand casting. Haider and Mufti [19] showed that mechanical properties (UTS, hardness) of squeezed Al-4% Cu alloy were mainly controlled by pouring and die temperature. In another investigation, it was deliberated that UTS and hardness were mainly influenced by squeeze pressure. It was also cited that die temperature and melt temperature has a little contribution towards controlling the magnitude of UTS and hardness during squeeze casting of AA2017 [20].

Patel et al. [21] studied the impact of process variables on squeeze casting of LM20 aluminum alloy. It was concluded that S_p and its duration were most prominent parameters influencing SR and UTS. Gan et al. [22] claimed that mechanical properties of Al–Cu–Mg alloy were greatly improved through squeeze casting process. Moreover, it was noted that slow cooling rate resulted into poor mechanical properties and coarse grain structure. In another study conducted on squeeze casting of A413 aluminum alloy it was reported that squeeze pressure was the most influencing factor for UTS and hardness [23]. Maximum value of UTS and hardness were obtained at S_p of 140 MPa, D_T of 225 °C, and P_T of 725 °C. Yaseen et al. [24] witnesses that mechanical properties of Al-Si-4% Cu alloy were expressively improved through squeeze casting process. Hardness of casted alloy improved with the rise in the value of squeeze pressure and pouring temperature. Souissi et al. [25] observed that UTS, micro-hardness, and yield strength were greatly influenced by squeeze pressure, followed by melt temperature during squeeze casting of AA2017 wrought aluminum alloy. Improved mechanical properties and fine grain structure were found by Azhagan et al. [26] using higher value of pressure during squeeze casting of AA6061 aluminum alloy. Guan et al. [27] showed that UTS and percent elongation of squeeze casted A356 aluminum alloy were enhanced about 12% and 21%, respectively as compared with the conventionally casted A356 aluminum alloy. Maximum value of UTS was found at 232 MPa S_p .

Manjunath et al. [28] studied the mechanical properties of squeeze casted LM2 aluminum alloy (Al-Si-Cu-Mg) using response surface methodology (CCD). The developed model was observed to have reasonable prediction accuracy. In another work conducted on the same material, it was explained that higher value of squeeze pressure improves the surface quality [29]. It was also found that die temperature has a negative relation with surface roughness and mechanical properties of the alloy.

From the literature, it has been found that the potential of squeeze casting process has not been comprehensively explored so far, as for casting of AA2026 aluminum alloy which is the primary focus of this research. Furthermore, the impact of squeeze casting parameters on surface roughness and mechanical properties of squeeze casted AA2026 are investigated in detail using response surface methodology which has not been examined before. It is pertinent to mention that the aspect of surface roughness of squeeze casted AA2016 aluminum alloy was given less attention than was given due consideration in the present study. Moreover, mathematical models for accurate prediction of surface roughness, UTS and hardness of squeeze casted AA2026 aluminum alloy have also been developed using response surface methodology. In addition to that, desirability analysis has been carried out to develop an optimal setting of control variables to simultaneously optimize all the selected response attributes.

2 Material and methods

AA2026 aluminum alloy has been selected as the casting material for the present work. Chemical composition of AA2026 aluminum alloy is given in Table 1. Spectrometry technique was used to validate the chemical composition of the material before experimentation.

Three input parameters: squeeze pressure (S_p), die temperature (D_T), and pouring temperature (P_T) with three levels of each have been selected. The selection criteria of input parameters are based on their significant influence on surface finish and mechanical properties [10, 15, 29]. The selection of input parameter limits is based on trial runs so that defect-free casted billet can be produced as followed by [19, 30]. Input parameters and their limits are shown in Table 2. Several methodologies like Taguchi method, gray rational analysis, response surface methodology, and simple statistical analysis have been applied by researchers during squeeze casting of aluminum

Table 1 Chemical composition of 2026 Al alloy

Elements	Al	Cu	Mn	Mg	Si	Ti	Fe
Weight %	93.96	3.91	0.72	1.23	0.06	0.04	0.08

Table 2 Squeeze casting input parameters and their respective limits

Input parameters	Units	Levels		
		Low (-1)	Medium (0)	High (+1)
Squeeze pressure (A)	MPa	70	100	130
Die temperature (B)	°C	200	225	250
Pouring temperature (C)	°C	750	790	830

alloys [15, 16, 19, 21]. However, RSM is found as the best modeling technique to forecast and optimize the output parameters with optimum combination of input parameters [28, 30–33]. RSM with central composite design is used for experimental design matrix. A total of nineteen experiments have been performed. The number of experiments is calculated by Eq. (1) [31]:

$$n = 2^k + 2k + m \tag{1}$$

where, *n* represents the number of experiments, *k* indicates the number of input parameters, and *m* describes the number of center points. Experimental design matrix with output responses has been given in Table 3.

Experimentation was performed on vertical hydraulic press with a capacity of 100 on. Electric resistance furnace with extreme temperature limit of 1200 °C at 5 KW was used for melting the material while oxyacetylene torch was used to achieve the required die temperature. Infrared thermometer (S-S: AR330) was employed to verify the die temperature.

Table 3 ANOVA for surface roughness

Source	Sum of squares	Df	Mean square	F value	p value	
Model	2.12	9	0.24	128.36	0.0001	Significant
A-squeeze pressure	1.61	1	1.61	877.06	< 0.0001	Significant
B-die temperature	0.16	1	0.16	84.60	< 0.0001	Significant
C-pouring temperature	0.01	1	0.01	8.12	0.0191	Significant
AB	0.02	1	0.02	9.33	0.0137	Significant
AC	0.08	1	0.08	44.73	< 0.0001	Significant
BC	0.11	1	0.11	58.96	< 0.0001	Significant
A ²	0.12	1	0.12	66.12	< 0.0001	Significant
B ²	0.00	1	0.00	1.04	0.3343	Not significant
C ²	0.01	1	0.01	4.12	0.0729	Not significant
Residual	0.02	9	0.00			
Lack of fit	0.01	5	0.00	3.78	0.1108	Not significant
Pure error	0.00	4	0.00			
Cor. total	2.13	18				
Std. dev.	0.04			R-squared		0.9923
Mean	1.26			Adj R-squared		0.9845
C.V. %	3.41			Pred R-squared		0.9488
PRESS	0.11			Adeq precision		40.916

The flow diagram depicting the squeeze casting process is shown in Fig. 1. Samples for UTS were prepared according to ASTM E8/E8M-11 standard. Tensile tests were performed using material testing system (MTS-810) having a capacity of 100 KN. For hardness measurement Rockwell hardness tester was used to measure the hardness at F scale by applying 60 kg load with 1/8-in the diameter ball. Surface roughness is measured by surface roughness tester (SJ-410). For each experimental run, three reading of responses were taken, and their average was considered as final.

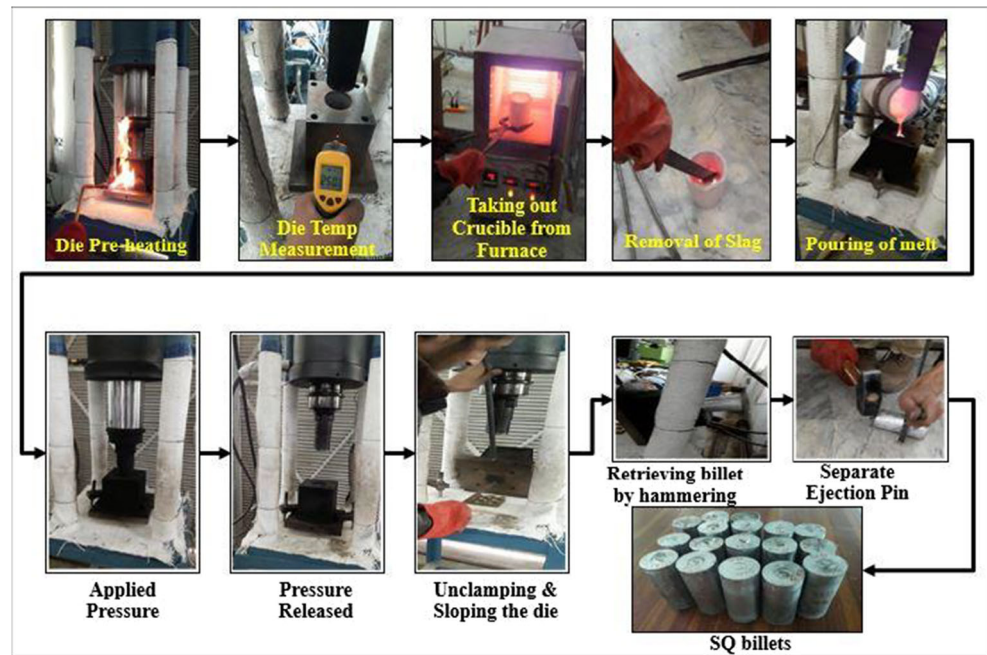
3 Results and discussion

Experimentation was successfully performed under DOE. After that surface roughness, UTS, and hardness of each sample was carefully measured. Results achieved after careful experimentation are then analyzed using various statistical tests and scanning electron microscopic analysis. The details and accompanying discussion pertaining to the aforesaid analysis techniques are presented in below sections.

3.1 Parametric significance analysis

ANOVA analysis has been performed in order to gauge the statistical significance of the control parameters for the three response attributes which means that any control parameter having a *p* value lesser than 0.05 would have a significant impact on the selected response attribute. Analysis has been

Fig. 1 Squeeze casting flow diagram



performed at a confidence interval of 95%. The results of the analysis are presented in Tables 3, 4, and 5. Based on the results of ANOVA for surface roughness, it has been noticed that factors A (S_p), B (D_T), C (P_T), AB , AC , BC , and A^2 have p values less than 0.05. This indicates that these control parameters have a significant role in determining the magnitude of surface roughness of squeeze casted AA2026 alloy. However, the contribution of squeeze pressure is the largest

one amongst the significant parameters in controlling the value of SR. In the case of UTS and hardness, A (S_p), B (D_T), C (P_T), A^2 , B^2 , and C^2 have come out to be the prominent model terms as their p values are less than the defined alpha value (0.05). But for both the said responses, it has been observed that pouring temperature (P_T) holds a leadingly high percentage contribution as compared with the other significant terms.

Table 4 ANOVA for ultimate tensile strength

Source	Sum of squares	Df	Mean square	F value	p value	
Model	14,532.03	9	1614.67	40.08	< 0.0001	Significant
A-squeeze pressure	2802.49	1	2802.49	69.56	< 0.0001	Significant
B-die temperature	1768.46	1	1768.46	43.89	< 0.0001	Significant
C-pouring temperature	3229.10	1	3229.10	80.15	< 0.0001	Significant
AB	10.13	1	10.13	0.25	0.6282	Not significant
AC	66.12	1	66.12	1.64	0.2322	Not significant
BC	1.13	1	1.13	0.03	0.8710	Not significant
A^2	4955.09	1	4955.09	122.99	< 0.0001	Significant
B^2	2385.29	1	2385.29	59.20	< 0.0001	Significant
C^2	817.54	1	817.54	20.29	0.0015	Significant
Residual	362.60	9	40.29			
Lack of fit	315.80	5	63.16	5.40	0.0637	Not significant
Pure error	46.80	4	11.70			
Cor. total	14,894.63	18				
Std. dev.	6.35			R-squared		0.9757
Mean	242.42			Adj R-squared		0.9513
C.V. %	2.62			Pred R-squared		0.8329
PRESS	2488.42			Adeq precision		19.423

Table 5 ANOVA for hardness

Source	Sum of squares	Df	Mean square	<i>F</i> value	<i>p</i> value	
Model	381.31	9	42.37	28.59	< 0.0001	Significant
A-squeeze pressure	14.03	1	14.03	9.47	0.0132	Significant
B-die temperature	22.69	1	22.69	15.32	0.0035	Significant
C-pouring temperature	79.74	1	79.74	53.82	< 0.0001	Significant
AB	0.45	1	0.45	0.30	0.5945	Not significant
AC	0.00	1	0.00	0.00	0.9775	Not significant
BC	0.66	1	0.66	0.45	0.5209	Not significant
A ²	176.25	1	176.25	118.95	< 0.0001	Significant
B ²	125.12	1	125.12	84.44	< 0.0001	Significant
C ²	13.50	1	13.50	9.11	0.0145	Significant
Residual	13.34	9	1.48			
Lack of Fit	9.24	5	1.85	1.80	0.2941	Not significant
Pure Error	4.10	4	1.03			
Cor total	394.65	18				
Std. dev.	1.22			R-squared		0.9662
Mean	86.25			Adj R-squared		0.9324
C.V. %	1.41			Pred R-squared		0.8056
PRESS	76.73			Adeq precision		14.855

3.2 Surface plot analysis

After examining the statistical significance of the control parameters and their interaction terms, surface plot analysis has been performed. 3D surface plots are used to graphically visualize the simultaneous impact of two input parameters on the selected output response [34]. These plots have been drawn on Design expert (7.0.0™). In these plots, three axes are used; one is of the response whereas the remaining two are for the input parameters. The rest of the selected parameters were kept constant at middle level. As in the present study, three input variables are involved therefore in all the surface plots; the third control factor is kept constant at its middle value. The results of the analysis are presented in Fig. 2. The influence of squeeze pressure and die temperature on SR is shown in Fig. 2a. When squeeze pressure is increased from low to high value, it has portrayed an inverse nonlinear behavior with SR as depicted by Vijian and Arunachalam [10]. Better surface quality is obtained at high value of squeeze pressure. This attributed to the fact that higher magnitude of S_p yields a fine microstructure because solidification occurs under high pressure. This also minimizes the chance of entrapment of gases into the melt which consequently lead to a decrease in the surface micro-cracks density. Both the said aspect results into a smoother surface finish of the casted part. The surface roughness profiles obtained from squeeze casted samples also demonstrate that at higher S_p , less irregularities is observed on the casted surface as depicted in Fig. 3. SEM micrographs taken for the two samples, i.e., one at lower S_p and the other at higher S_p also witnessed the same, presented

in Fig. 4. The surface texture produced on the later sample shows comparably a fine finish. However, a decrease in die temperature from low to high value results into a decrease in the value of SR. The same was also witnessed regarding the effect of die temperature in another work cited in the field of squeeze casting [26]. From Fig. 2b, it is obvious that when squeeze pressure is increased from low to high value, the SR is decreased while in the case of pouring temperature, SR got reduced by reducing the pouring temperature from low to medium value and afterwards reduction in P_T upsurges the SR magnitude. Figure 2c demonstrates the impact of die and pouring temperature on SR. It has been observed that a higher value of die temperature and pouring temperature is suited for lowering the surface roughness. In other words, these parameters have an inverse but slightly linear relationship with SR. The primary reason for this trend is high fluidity of the melt at larger value of both the temperatures which is likely to provide a smoother surface [27].

Figure 2d depicts the influence of squeeze pressure and die temperature on UTS. When squeeze pressure is boosted from low to high magnitude, the value of UTS increased up to medium level and then decreased at high value of squeeze pressure. Similarly, a rise in die temperature from low to high value, the value of UTS is increased because of constant heat transfer and low cooling rate. Alike trends of afore mentioned control parameters have also been reported by Shoaib et al. [30]. From Fig. 2e, it is evident that when squeeze pressure is increased from low to high value, the resulting UTS is also improved up to a certain rise in S_p but a little decrease in UTS has been found at highest value of pressure. The primary

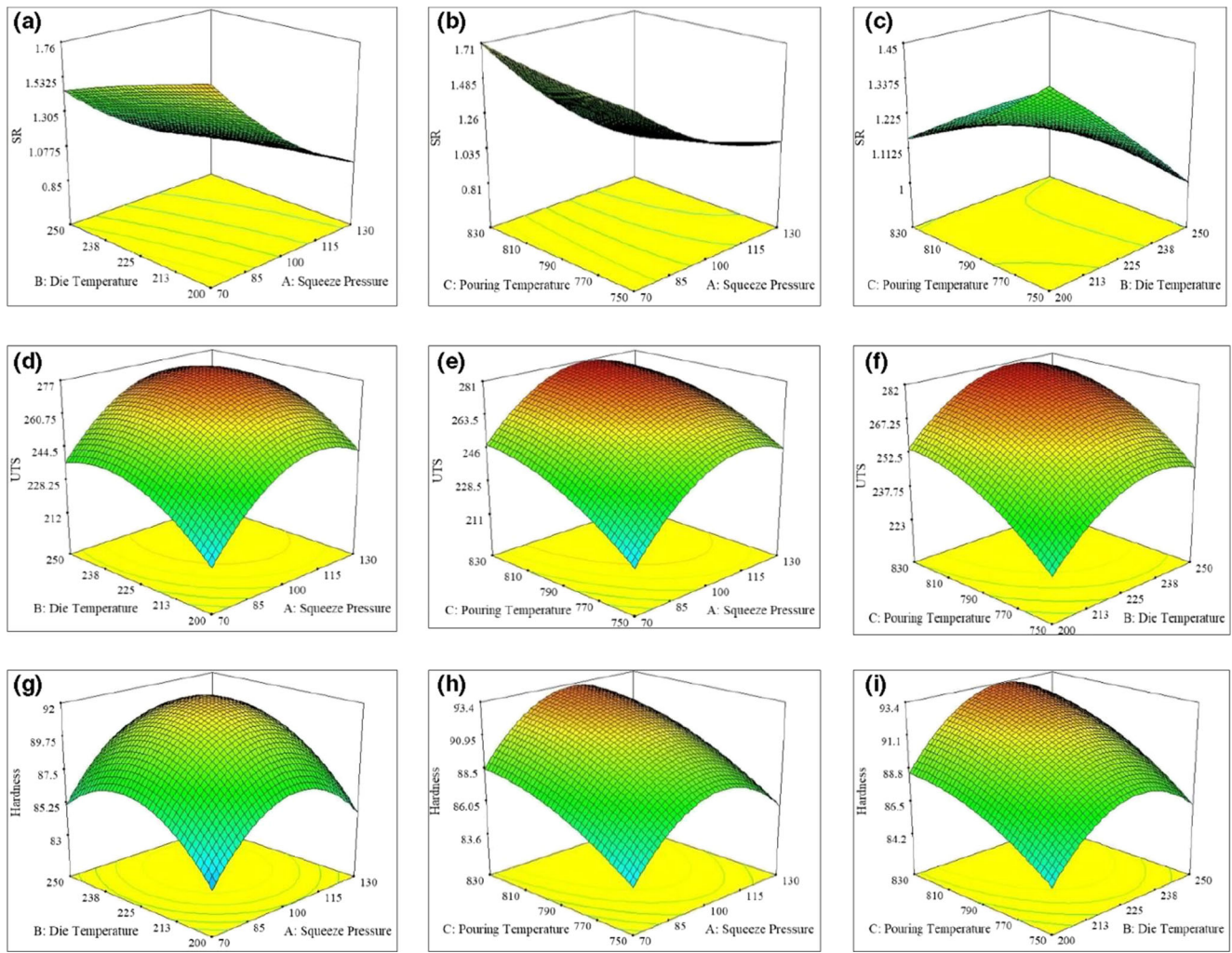


Fig. 2 Surface plot for SR: **a** die temperature vs squeeze pressure, **b** squeeze pressure vs pouring temperature, and **c** die temperature vs pouring temperature. Surface plot for UTS: **d** die temperature vs squeeze pressure, **e** pouring temperature vs squeeze pressure, and **f**

pouring temperature vs die temperature. Surface plot for hardness: **g** pouring temperature vs squeeze pressure, **h** temperature vs squeeze pressure, and **i** pouring temperature vs die temperature

reason for this shift is the change in the grain structure. Actually, higher squeeze pressure promotes the formation of coarse grains structure that ultimately resulted into a reduction in the magnitude of UTS. Yue et al. [35] also witnessed the same. In the case of pouring temperature, UTS is improved by raising the pouring temperature from low to high value. Figure 2f enlightens the impact of die temperature and pouring temperature on UTS. It is manifest that as die and pouring

temperatures are increased, the UTS of the squeeze samples are also enhanced. Basically, to achieve better UTS of the casted product, it is essential that premature solidification should not occur. Therefore, larger value of both the temperatures, i.e., D_T and P_T provides a better ultimate tensile strength as the chance of premature solidifications are minimized because both melt and die has a sufficiently high temperature [27]. Fractography of fractured tensile samples was

Fig. 3 Roughness profiles; **a** At low S_p and **b** at high S_p

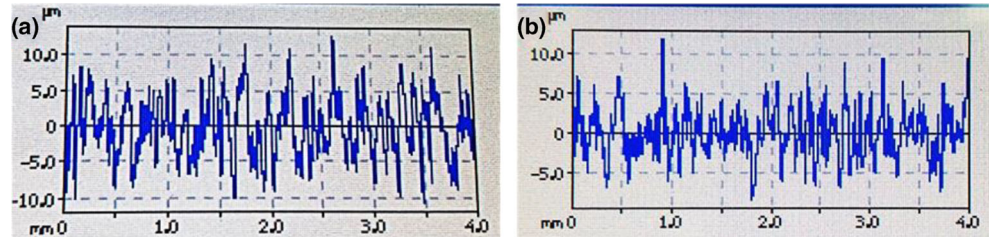
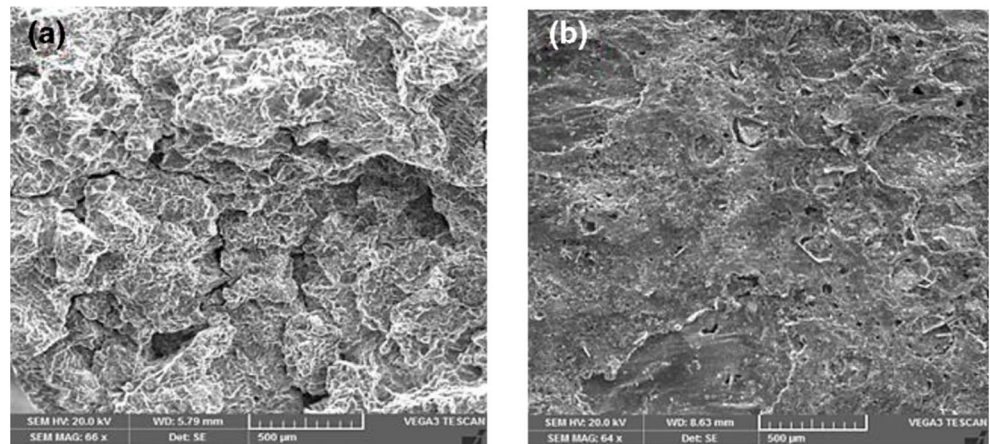


Fig. 4 SEM micrographs of squeeze casted AA2026 samples: **a** At low S_p and **b** at high S_p



examined using scanning electron microscope (VEGA3-SEM). SEM images clearly revealed that fracture occurred in intergranular manner and indicated cleavage fracture for run no. 7, whereas, dimple fracture observed for run no. 13 and 14, where fractured occurred in a transgranular manner (Fig. 5).

Figure 2g shows the effect of squeeze pressure and die temperature on hardness. Increase in the value of squeeze pressure improves the hardness of the casted product up to a certain limit but beyond that limit, hardness value got reduced. This is due to the formation of micro-cracks that resulted into lower hardness value. On the same analogy, rise in die temperature from low to high value, the value of hardness increased up to certain point then it is decreased with the further rise in die temperature. Identical trends have been reported by Shoaib et al. [30]. From Fig. 2h, it is obvious that when squeeze pressure is increased from low to high value, the hardness is increased up to a certain point afterwards; a little decrease in hardness has been observed which is due to the formation of shrinkage

porosities and micro-cracks. In the case of pouring temperature, hardness is increased by increasing the pouring temperature from low to high value. Similarly quoted by Patel et al. [14]. Figure 2i depicts the impact of die temperature and pouring temperature on hardness. It is clear from the figure that a rise in die temperature resulted into an abrupt increase in the magnitude of hardness up to a certain limit and beyond that it reduces once again. The trend portrayed pouring temperature are also found to be identical with die temperature with respect to the hardness.

3.3 Contour plot analysis

Contour plots are used to find the optimal combination of input parameters for achieving the optimal value of the selected response parameter. These plot have been drawn on Design expert (7.0.0™). In these plots, the contours of the response characteristic are developed considering two control variables at a time. The values of the response are mentioned against each contour of the selected response. Based on the desired

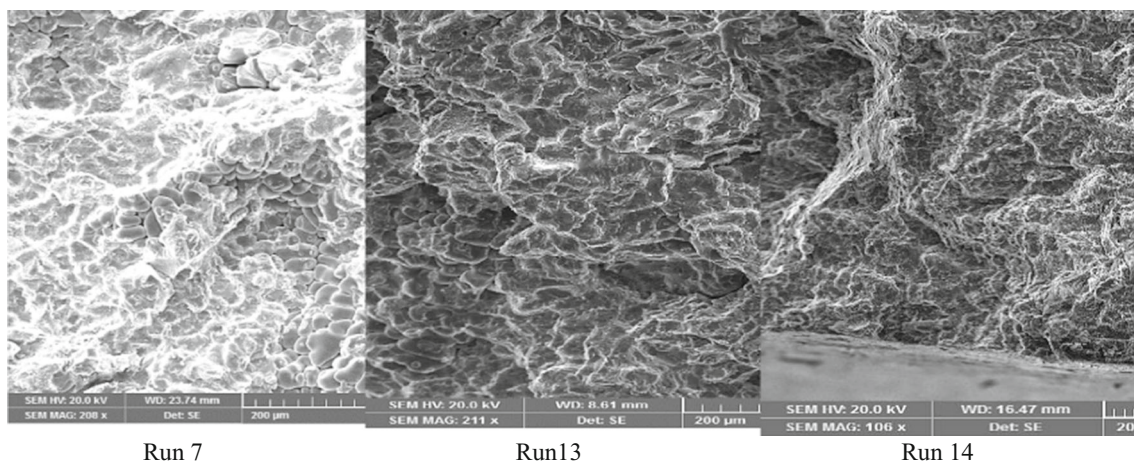


Fig. 5 SEM images of tensile fracture surface for experimental run (7, 13, and 14)

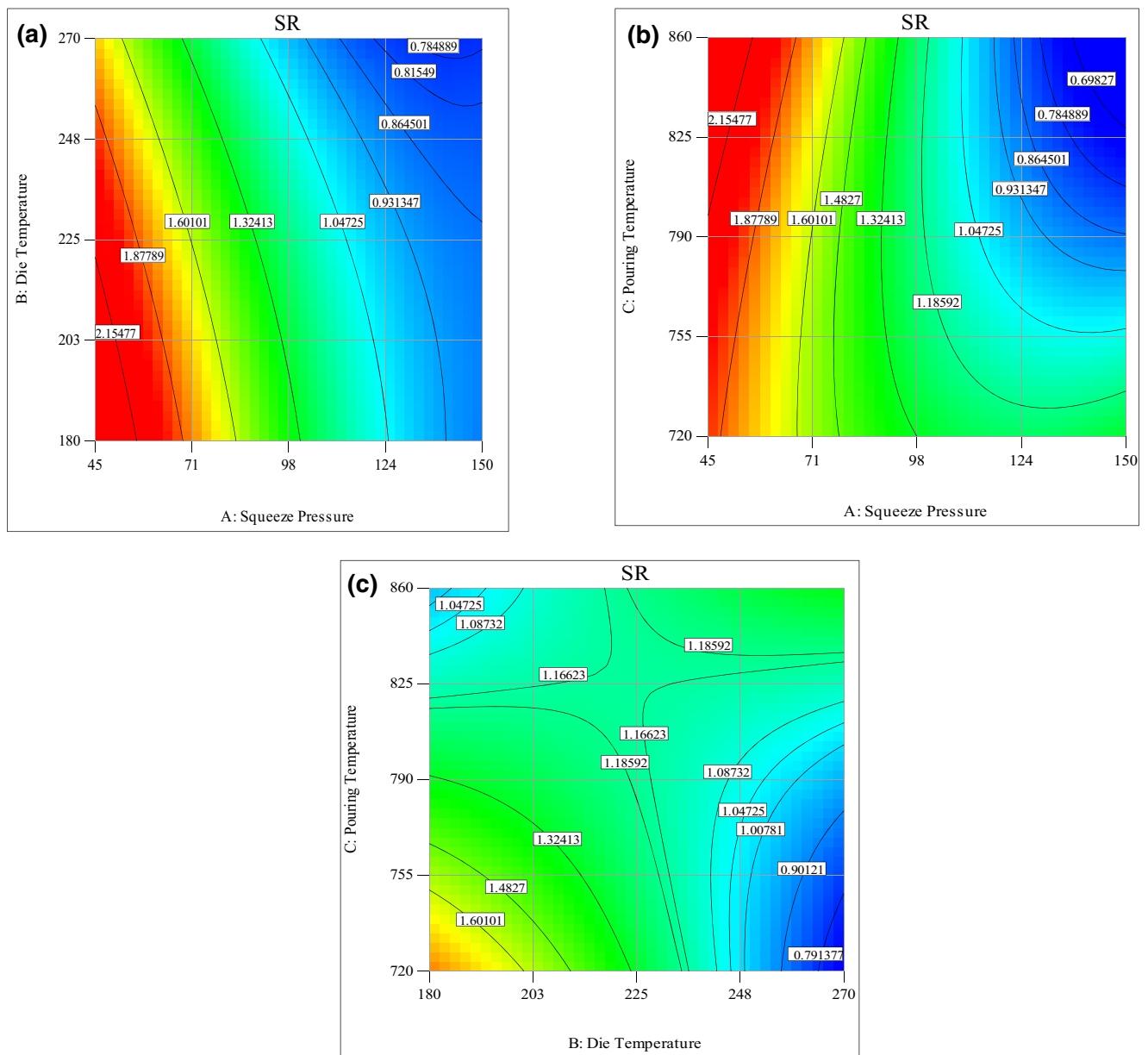


Fig. 6 **a** Contour plot for SR, die temperature vs squeeze pressure. **b** Contour plot for SR, pouring temperature vs squeeze pressure. **c** Contour plot for SR, die temperature vs pouring temperature

value of the response optimal values of the two input parameters are identified while the rest of the control parameters were kept constant at their middle level. The results of the analysis are presented in Fig. 6. It has been noted that optimize value of SR ($0.78 \mu\text{m}$) is obtained at squeeze pressure ranges between 130 and 150 MPa and die temperature $250\text{--}270 \text{ }^\circ\text{C}$ as shown in Fig. 6a. Optimized value of SR ($0.69 \mu\text{m}$) is obtained at squeeze pressure ranges between 140 and 150 MPa and pouring temperature $830\text{--}850 \text{ }^\circ\text{C}$ as shown in Fig. 6b. Optimized value of SR ($0.79 \mu\text{m}$) is achieved at die temperature ranges between 260 and $270 \text{ }^\circ\text{C}$ and pouring temperature $720\text{--}730 \text{ }^\circ\text{C}$ as shown in Fig. 6c. Figure 7a depicts that

optimized value of UTS (275.91 MPa) is obtained at squeeze pressure ranges between 110 and 120 MPa and die temperature $230\text{--}240 \text{ }^\circ\text{C}$. Optimized value of UTS (280.49 MPa) is obtained at squeeze pressure ranges between 110 and 120 MPa and pouring temperature $820\text{--}830 \text{ }^\circ\text{C}$ as highlighted in Fig. 7b. Optimized value of UTS (281.06 MPa) is achieved at die temperature ranges between 230 and $240 \text{ }^\circ\text{C}$ and pouring temperature $820\text{--}830 \text{ }^\circ\text{C}$ as demonstrated in Fig. 7c. Figure 8a depicts that optimize value of hardness (91.88 HRF) is obtained at squeeze pressure ranges between 100 and 110 MPa and die temperature $230\text{--}240 \text{ }^\circ\text{C}$. Optimized value of hardness (93.22 HRF) is obtained at squeeze pressure

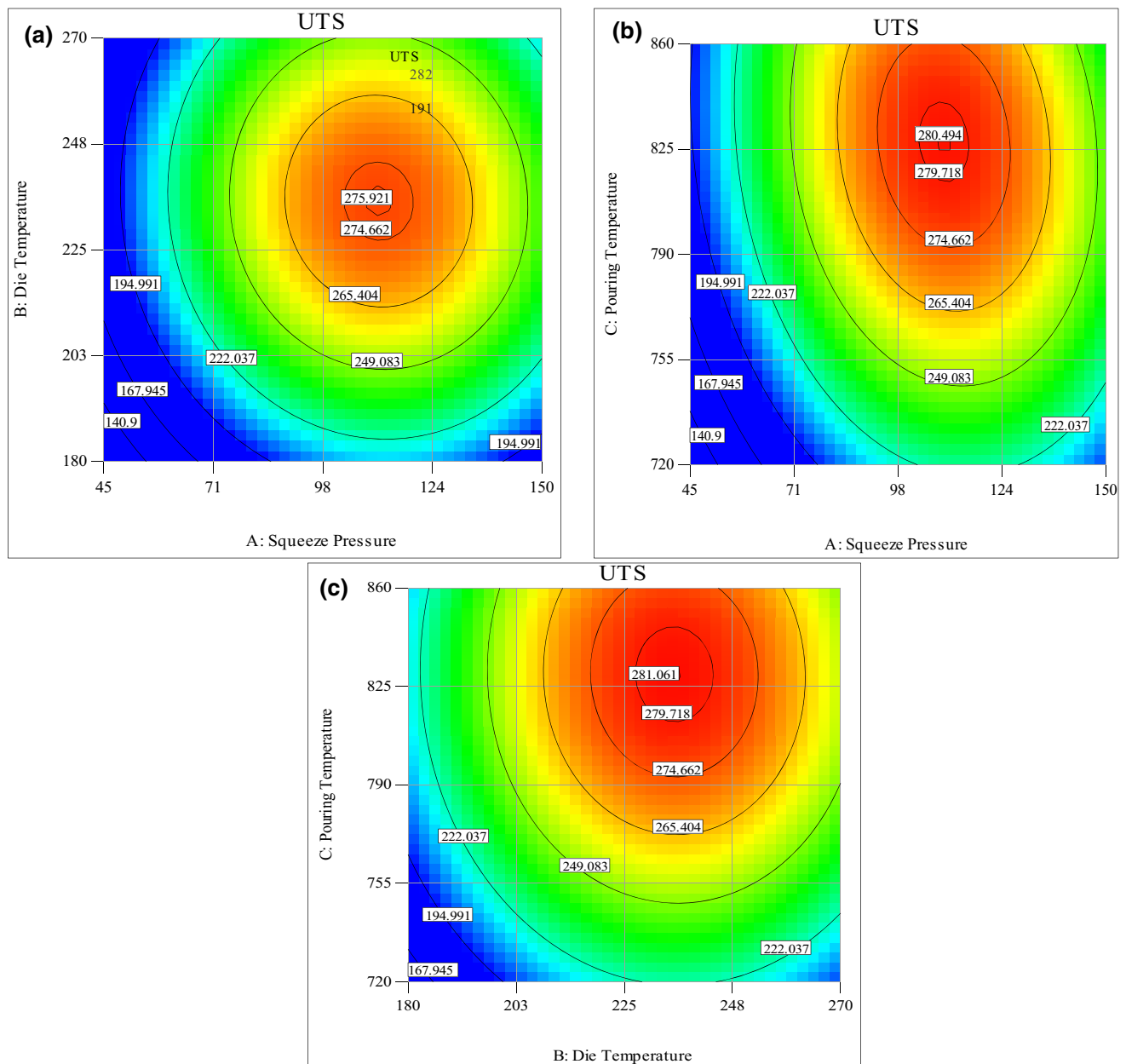


Fig. 7 a Contour plot for UTS, die temperature vs squeeze pressure. b Contour plot for UTS, pouring temperature vs squeeze pressure. c Contour plot for UTS, die temperature vs pouring temperature

ranges between 100 and 110 MPa and pouring temperature 830–840 °C as described in Fig. 8b. Optimized value of hardness (93.411 HRF) is achieved at die temperature ranges between 230 and 240 °C and pouring temperature 840–850 °C which is evident in Fig. 8c.

3.4 Mathematical modeling

In addition to finding out the optimal ranges of the control parameters for the selected response attributes, mathematical models are also developed. Based on the experimental

results and statistical tests, it has been noted that quadratic relationship is the best fit model for all the responses, i.e., SR, UTS, and hardness. The proposed mathematical models are described by Eqs. 2–4. Analysis of variance also validates the adequacy of the proposed models as the *p*-values for the models are lesser than the defined alpha value as shown in Tables 3, 4, and 5. The models’ fit summary provided in Tables 3, 4, and 5 clearly demonstrate that value of R-sq adjusted is more than 90% for all the models which is the proof that model explains the process variation in fairly good manner.

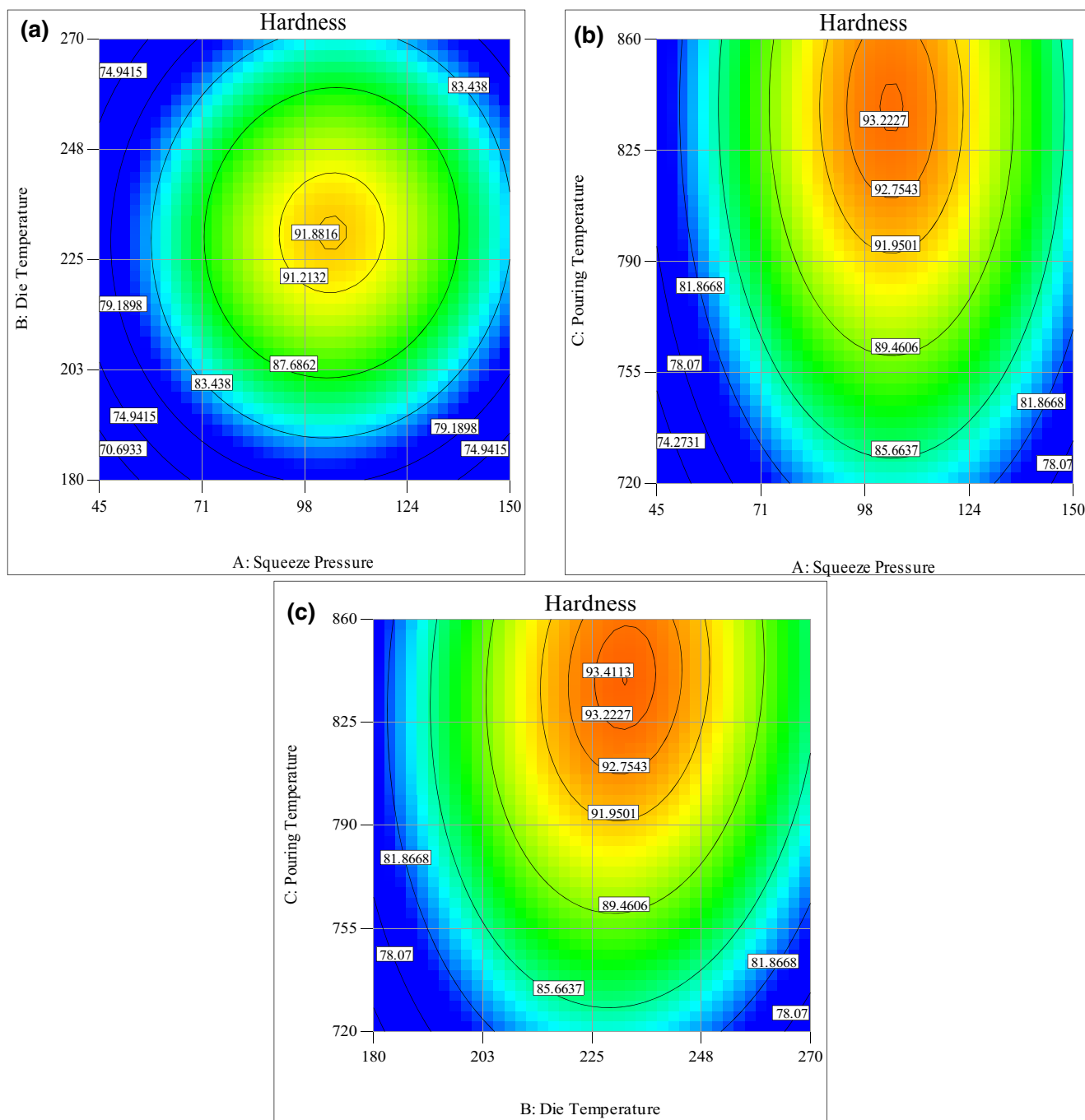


Fig. 8 **a** Contour plot for hardness, die temperature vs squeeze pressure. **b** Contour plot for hardness, pouring temperature vs squeeze pressure. **c** Contour plot for Hardness, die temperature vs pouring temperature

$$\begin{aligned}
 SR = & +28.59 + (0.02 \times A) - (0.09 \times B) - (0.04 \times C) \\
 & + (6.17 \times 10^{-5} \times AB) - (8 \times 10^{-5} \times AC) \\
 & + (1.16 \times 10^{-5} \times BC) \\
 & + (1.05 \times 10^{-5} \times A^2) - (1.89 \times 10^{-5} \times B^2) \\
 & + (1.47 \times 10^{-5} \times C^2)
 \end{aligned} \tag{2}$$

$$\begin{aligned}
 UTS = & -4773.48 + (6.94 \times A) + (10.42 \times B) \\
 & + (8.35 \times C) - (1.5 \times 10^{-4} \times AB) - (2.39 \times 10^{-4} \times AC) \\
 & + (3.75 \times 10^{-5} \times BC) - (2.12 \times 10^{-3} \times A^2) \\
 & - (2.11 \times 10^{-3} \times B^2) - (4.83 \times 10^{-4} \times C^2)
 \end{aligned} \tag{3}$$

Table 6 Validation results

Runs	Input Parameters			Actual values of output response			Predicted values of output response			% Error		
	A (MPa)	B (°C)	C (°C)	SR (µm)	UTS (MPa)	Hardness (HRF)	SR (µm)	UTS (MPa)	Hardness (HRF)	SR (µm)	UTS (MPa)	Hardness (HRF)
1												
2	110	210	800	1.05	266	90.68	1.09	265.65	90.25	3.7	0.1	0.5
3	80	240	825	1.5	262.87	87.59	1.47	264.69	90.55	2.0	0.7	3.3
4	110	240	800	1.04	275.21	89	1.02	278.75	91.98	2.0	1.3	3.2
5	80	240	825	1.42	261.98	91.38	1.47	264.69	90.55	3.4	1.0	0.9

$$\begin{aligned}
 \text{Hardness} = & -586.71 + (0.77 \times A) + (1.97 \times B) + (0.98 \times C) \quad (4) \\
 & + (3.17 \times 10^{-4} \times AB) - (1 \times 10^{-5} \times AC) \\
 & + (2.88 \times 10^{-4} \times BC) - (3.99 \times 10^{-3} \times A^2) \\
 & - (4.84 \times 10^{-3} \times B^2) - (6.2 \times 10^{-4} \times C^2)
 \end{aligned}$$

Table 7 Constraints values for input parameters and responses

Input parameters	Goal	Lower limit	Upper limit
Squeeze pressure (MPa)	In range	70	130
Die temperature (°C)	In range	200	250
Pouring temperature (°C)	In range	750	850
Responses			
SR (µm)	Minimize	0.72	2.01
UTS (MPa)	Maximize	191	282
Hardness (HRF)	Maximize	80.3	94.8

3.5 Confirmatory tests

The accuracy of the developed model has not only been tested through statistical means rather five confirmatory experiments are also performed. The results of these experiments are provided in Table 6. %. The following equation [36] is used to find out the models’ prediction error. It is encouraging to note that percentage error between actual and predicted values is less than 5% which in turns highlight the validity of the developed models.

$$\% \text{Error} = |(\text{Actual quantity} - \text{Predicted quantity}) / \text{Predicted quantity}| \times 100 \quad (5)$$

4 Multi-objective optimization

Optimal levels of input parameters (S_p , D_T , and P_T) are essential for minimizing SR while maximizing UTS and hardness concomitantly for manufacturing purpose. Multi-response

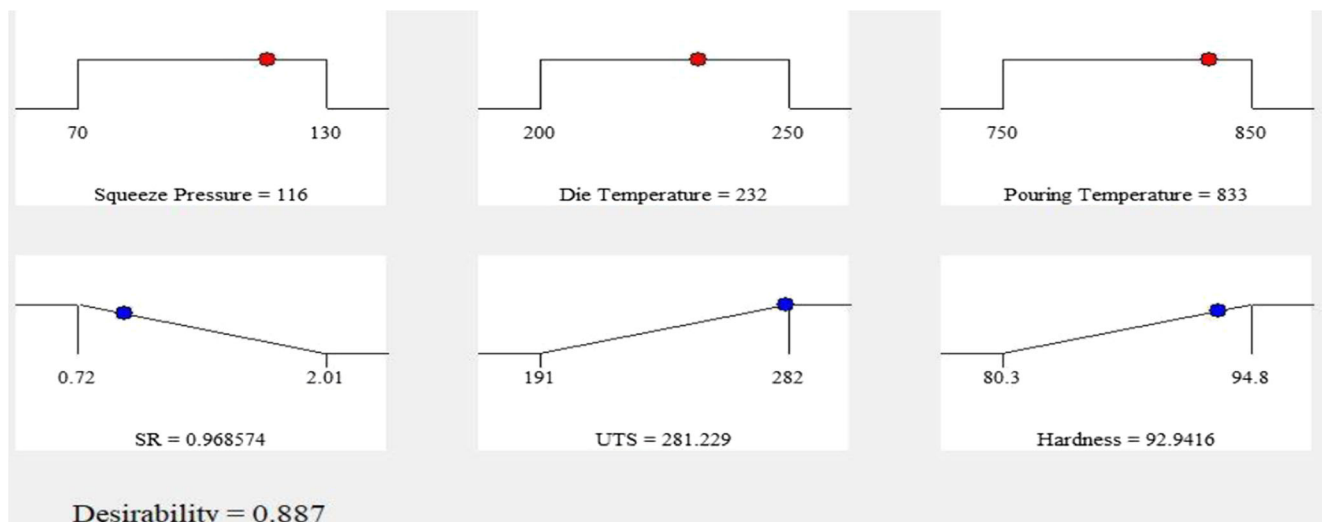
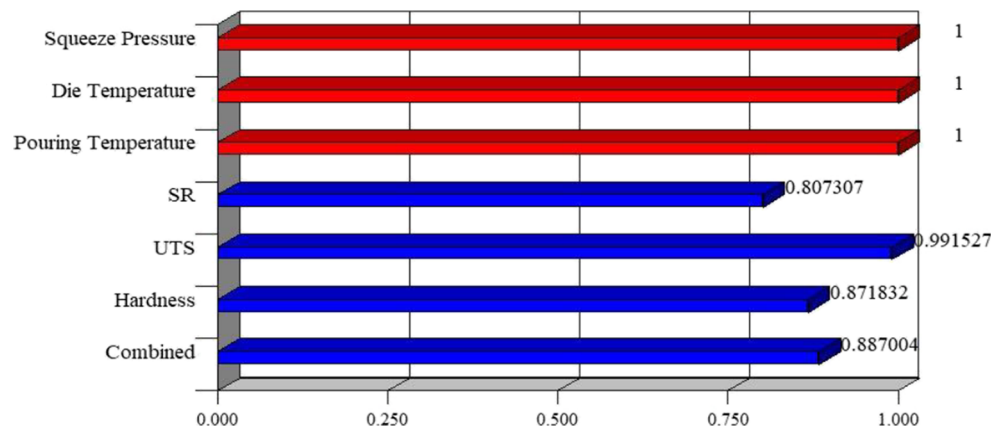


Fig. 9 Optimal values for input parameters and responses with compound desirability

Fig. 10 Compound desirability bar graph



optimization is best method to obtain optimal results for conflicting responses. Desirability is an easy method for the optimization of conflicting responses simultaneously [37]. In this method desirability function is employed whose value ranges from 0 to 1 (least to most desirable) for the transformation of estimated responses into desirability values called range-free values. First of all, desirability function is developed afterwards objective function as well as compound function are calculated through weighted geometric mean for all range-free values [38, 39]. Optimal levels of input parameters have been obtained for optimization of conflicting responses simultaneously by using developed mathematical models of SR, UTS and hardness. Constraints values of input parameters and predicted values of responses have been provided in Table 7. RSM-based desirability approach suggests that all the three selected responses are simultaneously optimized if input parameters are selected in such a way that $S_p = 116$ MPa, $D_T = 232$ °C, and $P_T = 833$ °C. These settings ensure a minimum value of SR (0.968) and maximum value of UTS (281 MPa) and hardness (92.94) as shown Fig. 9. Figure 10 depicts that the desirability values of SR, UTS, and hardness are 80.7%, 99.15%, and 87.18%, respectively. The value of combined desirability has also been found to be reasonably high, i.e., 88.7% which is actually highlighting the adequacy of the proposed model.

5 Conclusions

The present research is aimed at envisaging the potential of squeeze casting process for casting of Al AA2026 alloy which is commonly used in aerospace and automotive industry. The effect of key parameters of squeeze casting process namely; S_p , D_T , and P_T on surface quality and mechanical properties (UTS and hardness) of squeeze casted AA2026 aluminum alloy has been examined thoroughly using response surface methodology (CCD). Experimental results are then examined using various statistical tests and SEM analysis. Based on the

results and their discussion following conclusions may possibly be drawn:

- Squeeze pressure is observed to be the most influencing input parameter for surface roughness followed by die temperature and pouring temperature. However, in the case of UTS and hardness, pouring temperature is most contributing factor.
- Surface plot analysis depicts that there exists an inverse and nonlinear relationship between surface roughness and S_p whereas the remaining two control variables assume an inverse and slightly linear relation with the aforesaid response attribute. But in the case of UTS and hardness, squeeze pressure has shown an increasing nonlinear trend while die temperature and pouring temperature have also portrayed a nonlinear increasing relation.
- SEM analysis of the fractured sample of squeeze casted AA2026 shows that cleavage fracture and dimple fracture are the two modes of fracture. The former fracture occurred in intergranular manner whereas the later occur in transgranular manner.
- Mathematical models are developed for all the response characteristics. Quadratic relationship is found to be the best fit model for all the three responses. The developed models' adequacy has also been validated through confirmatory tests. Results of confirmatory trials have shown that the proposed models have high degree of prediction accuracy. Additionally, ANOVA has also proved the statistical significance of the proposed models.
- Optimal settings of control variables for individual optimization of selected responses are achieved using contour plots technique. It has been revealed that improved surface quality is found at S_p of 130–150 MPa, D_T of 250–270 °C, and P_T of 830–850 °C. Maximum value of UTS is achieved at S_p of 110–120 MPa, D_T of 230–240 °C, and P_T of 820–830 °C. Optimal value of hardness is obtained at S_p of 100–110 MPa, D_T of 230–240 °C, and P_T of 830–850 °C.

- In addition to the individual optimization of the responses, optimal settings of control factors for simultaneous optimization of surface roughness, UTS, and hardness are also developed using desirability approach. According to this multi-response optimization approach optimal parametric combination that ensures the optimization of all the selected responses is S_p of 113 MPa, D_T of 232 °C, and P_T of 833 °C.

References

- Jorstad J, Apelian D (2009) Hypereutectic al-si alloys: practical casting considerations. *Int J Met* 3:13–36. <https://doi.org/10.1007/BF03355450>
- Sigworth G (2011) Understanding quality in aluminum castings. *Int J Met* 5:7–22. <https://doi.org/10.1007/BF03355504>
- Pratheesh K, Kanjirathinkal A, Joseph MA, Ravi M (2017) Study on the effects of squeeze pressure on mechanical properties and wear characteristics of near-eutectic Al-Si-cu-mg-Ni piston alloy with variable Cu content. *Int J Met* 11:831–842. <https://doi.org/10.1007/s40962-017-0132-0>
- Greß T, Mittler T, Schmid S, Chen H, Ben Khalifa N, Volk W (2018) Thermal analysis and production of as-cast Al 7075/6060 bilayer billets. *Int J Met*. <https://doi.org/10.1007/s40962-018-0282-8>
- Vijian P, Arunachalam VP (2007) Optimization of squeeze casting process parameters using Taguchi analysis. *Int J Adv Manuf Technol* 33:1122–1127
- Dursun T, Soutis C (2014) Recent developments in advanced aircraft aluminium alloys. *Mater Des* 56:862–871. <https://doi.org/10.1016/j.matdes.2013.12.002>
- Souissi N, Souissi S, Lecompte J-P, Amar MB, Bradai C, Halouani F (2015) Improvement of ductility for squeeze cast 2017 a wrought aluminum alloy using the Taguchi method. *Int J Adv Manuf Technol* 78:2069–2077
- Gupta KM (2014) *Engineering materials: research, applications and advances*. CRC Press
- Raj R, Thakur DG (2016) Qualitative and quantitative assessment of microstructure in Al-B4C metal matrix composite processed by modified stir casting technique. *Arch Civ Mech Eng* 16:949–960. <https://doi.org/10.1016/j.acme.2016.07.004>
- Vijian P, Arunachalam VP (2006) Optimization of squeeze cast parameters of LM6 aluminium alloy for surface roughness using Taguchi method. *J Mater Process Technol* 180:161–166
- Li Y, Yang H, Xing Z (2017) Numerical simulation and process optimization of squeeze casting process of an automobile control arm. *Int J Adv Manuf Technol* 88:941–947. <https://doi.org/10.1007/s00170-016-8845-4>
- Ghomashchi MR, Vikhrov A (2000) Squeeze casting: an overview. *J Mater Process Technol* 101:1–9
- Fan CH, Chen ZH, He WQ, Chen JH, Chen D (2010) Effects of the casting temperature on microstructure and mechanical properties of the squeeze-cast Al–Zn–mg–cu alloy. *J Alloys Compd* 504:L42–L45
- Patel GCM, Mathew R, Krishna P, Parappagoudar MB (2014) Investigation of squeeze cast process parameters effects on secondary dendrite arm spacing using statistical regression and artificial neural network models. *Procedia Technol* 14:149–156
- Patel GCM, Krishna P, Parappagoudar MB (2014) Optimization of squeeze cast process parameters using Taguchi and grey relational analysis. *Procedia Technol* 14:157–164
- Senthil P, Amirthagadeswaran KS (2012) Optimization of squeeze casting parameters for non symmetrical AC2A aluminium alloy castings through Taguchi method. *J Mech Sci Technol* 26:1141–1147
- Souissi S, Ben Amar M, Bradai C (2013) Microstructure characterization and tensile properties of direct squeeze cast and gravity die cast 2017A wrought Al alloy. *Int J Mater Form* 6:249–254
- Bin S, Xing S, Ning Z, Lan LI (2013) Influence of technical parameters on strength and ductility of AlSi9Cu3 alloys in squeeze casting. *Trans Nonferrous Metals Soc China* 23:977–982
- Haider KMA, Mufti NA (2014) Mechanical and microstructural evaluation of squeeze cast Al-4% Cu alloy using a full-factorial experimental design. *J Miner Met Mater Soc* 66:1446–1453
- Souissi N, Souissi S, Le Niniven C, Amar MB, Bradai C, Elhalouani F (2014) Optimization of squeeze casting parameters for 2017 a wrought al alloy using Taguchi method. *Metals (Basel)* 4:141–154
- Patel M, GC PK, Parappagoudar MB (2015) Modelling of squeeze casting process using design of experiments and response surface methodology. *Int J Cast Met Res* 28:167–180
- Gan Y, Zhang D, Zhang W, Li Y (2015) Effect of cooling rate on microstructure and mechanical properties of squeeze cast Al–Cu–Mg alloy. *Int J Cast Met Res* 28:50–58
- Soundararajan R, Ramesh A, Sivasankaran S, Sathishkumar A (2015) Modeling and analysis of mechanical properties of aluminium alloy (A413) processed through squeeze casting route using artificial neural network model and statistical technique. *Adv Mater Sci Eng* 2015:1–16
- Yaseen RS, Hussein HA, Jassim AH (n.d.) Study the effects of squeeze casting parameters on the corrosion behavior of Al-Si-4Cu alloy
- Souissi N, Souissi S, Le Niniven C, Amar MB, Bradai C, Halouani F (2015) An experimental design and theoretical analysis of squeeze casting parameters for 2017A aluminium alloy. *Int J Mater Eng Innov* 6:59–73
- Azhagan MT, Mohan B, Rajadurai A (2015) Experimental study of squeeze casting of aluminium alloy AA6061. *Appl Mech Mater Trans Tech Publ* 422–426
- Guan RG, Zhao ZY, Li YD, Chen TJ, Xu SX, Qi PX (2016) Microstructure and properties of squeeze cast A356 alloy processed with a vibrating slope. *J Mater Process Technol* 229:514–519
- Manjunath Patel GC, Krishna P, Parappagoudar MB (2016) Squeeze casting process modeling by a conventional statistical regression analysis approach. *Appl Math Model* 40:6869–6888
- Manjunath Patel GC, Krishna P, Parappagoudar MB (2016) Modelling and multi-objective optimisation of squeeze casting process using regression analysis and genetic algorithm. *Aust J Mech Eng* 14:182–198
- Sarfraz S, Jahanzaib M, Wasim A, Hussain S, Aziz H (2017) Investigating the effects of as-casted and in situ heat-treated squeeze casting of Al-3.5% Cu alloy. *Int J Adv Manuf Technol* 89:3547–3561
- Montgomery DC (2017) *Design and analysis of experiments*. Wiley, Hoboken
- Myers RH, Montgomery DC (1995) *Response surface methodology: process and product optimization using designed experiments*. Wiley, Hoboken
- Maeng DY, Lee JH, Won CW, Cho SS, Chun BS (2000) The effects of processing parameters on the microstructure and mechanical properties of modified B390 alloy in direct squeeze casting. *J Mater Process Technol* 105:196–203

34. Mia M, Dhar NR (2016) Prediction of surface roughness in hard turning under high pressure coolant using artificial neural network. *Measurement*. 92:464–474
35. Yue TM (1997) Squeeze casting of high-strength aluminium wrought alloy AA7010. *J Mater Process Technol* 66:179–185
36. Azam M, Jahanzaib M, Wasim A, Hussain S (2015) Surface roughness modeling using RSM for HSLA steel by coated carbide tools. *Int J Adv Manuf Technol* 78:1031–1041
37. Derringer G, Suich R (1980) Simultaneous optimization of several response variables. *J Qual Technol* 12:214–219. <https://doi.org/10.1080/00224065.1980.11980968>
38. El-Taweel TA (2009) Multi-response optimization of EDM with Al-Cu-Si-TiC P/M composite electrode. *Int J Adv Manuf Technol* 44:100–113. <https://doi.org/10.1007/s00170-008-1825-6>
39. Natarajan U, Periyaran PR, Yang SH (2011) Multiple-response optimization for micro-endmilling process using response surface methodology. *Int J Adv Manuf Technol* 56:177–185. <https://doi.org/10.1007/s00170-011-3156-2>

Publisher's note Springer Nature remains neutral with regard to jurisdictional claims in published maps and institutional affiliations.